

A novel method of microfabrication and manipulation of bacterial teamsters in low Reynolds number fluidic environments

Edward B. Steager · Jigarkumar A. Patel ·
Chang-Beom Kim · Dong Kee Yi ·
Woong Lee · Min Jun Kim

Received: 17 October 2007 / Accepted: 4 December 2007 / Published online: 20 December 2007
© Springer-Verlag 2007

Abstract The flagellated bacteria *Serratia marcescens* have been employed as fluidic actuators to propel custom designed microstructures through the use of a swarm blotting technique. The novel methodology for microfabrication, manipulation, and experimentation is described in detail, and the advantages and drawbacks of alternative techniques are considered. Our results with PDMS and silicon microstructures led to the discovery of SU-8 as a suitable material. A microstructure-tracking algorithm was developed to quantify the motion. The methodology is applied in a study of effects of microstructure geometry on velocity and trajectory in an open fluidic channel. Additionally, relationships between structure dimension and velocity are discussed.

Keywords Biomolecular motors · Flagellated bacteria · Microrobotics · Microactuation

1 Introduction

Recent developments in microfabrication technologies enabled a variety of miniaturized systems consisting of

micro-mixers, pumps and various other actuating systems. Due to the size and surface force effects (Ho and Tai 1998; Gal-El-Hak 1999), the microscale fluidic transport phenomena are different from their larger-scale counterparts, generally described by the Navier–Stokes equation (Eringen 1964). Hence, the technological demands on microfluidic systems require a better understanding of the flow characteristics in micron and sub-micron level devices. For devices smaller than 1 mm in length, the origin of the fluid forces can be created by the surface forces or body forces driven by pressures, based on short-range van der Waals forces and longer range electrostatic or Coulombic forces (Ho and Tai 1998; Gal-El-Hak 1999). One approach to manipulate fluids actuating with extremely high efficiency in low Reynolds number fluidic environments is to utilize bio-molecular motors from flagellated bacteria. Several research groups have initiated the study of microactuation techniques in fluidic environments using intact microorganisms as a power source. Substantial progress has been demonstrated in this area; however, the ability to integrate microstructures of customized design has been essentially absent. To enable the study of this type of microactuation, a method of microfabrication and manipulation is required to combine biological components with precisely designed microstructures.

Darnton et al. (2004) investigated and illustrated that auto-mobile chips made of polydimethylsiloxane (PDMS), once blotted with *S. marcescens*, could be propelled and move at a speed of approximately 5 $\mu\text{m/s}$. However, automobile chips were made in such a way that every chip was different in size and shape. This factor may affect the result and repeatability of the experiment. Microbeads, which are widely available commercially have also been used as microstructures and have been used to demonstrate control techniques for a number of research groups. The

E. B. Steager · J. A. Patel · C.-B. Kim · M. J. Kim (✉)
Department of Mechanical Engineering and Mechanics,
Drexel University, Philadelphia, PA 19104, USA
e-mail: mkim@coe.drexel.edu

D. K. Yi
Gachon Bionano Research Institute, Kyungwon University,
Sungnam 461-701, Republic of Korea

W. Lee
School of Nano and Advanced Materials Engineering,
Changwon National University, 9 Sarim-Dong,
Changwon, Gyungnam 641-773, Republic of Korea

bacteria *Magnetospirillum gryphiswaldense* has been used to manipulate 3 μm beads along preplanned paths using magnetotactic directional control (Martel et al. 2006). On/off motion control of 10 μm beads using *S. marcescens* has also been demonstrated using the addition of copper ions and/or ethylenediaminetetraacetic acid (EDTA) (Behkam and Sitti 2007). Additionally, the algae *Chlamydomonas reinhardtii* has served as a microactuator to move 6 μm beads using a combination of surface chemistry to attach loads, phototaxis to steer cells, and photochemistry to release loads (Weibel et al. 2005). Nonetheless, there are two distinct disadvantages of microbead use. Primarily, the study of actuation relies on the random interaction of the microorganisms with microbeads. Given a large number of organisms and an abundance of microbeads, the statistical chance of interaction is significant, but there is a lack of targeted manipulation and ensuing ability to intentionally vary experimental parameters with a great degree of certainty. Secondly, the ability to study the effect of loading on structures of varying geometry is lacking since the microbeads have a uniformly spherical shape.

For this study, the bacteria *S. marcescens* has been chosen due to its ability to exploit the swarming behavior that is apparent on soft agar surfaces. *S. marcescens* are peritrichously flagellated, gram negative bacteria which are roughly 2 μm long and 1 μm in diameter in their swimming form. *S. marcescens* swims at speeds of about 50 $\mu\text{m/s}$, propelled by the rotation of about five long (10 μm), thin (20 nm), helical filaments, each driven at its base by a flagellar motor (Berg 2003). The individual flagella are driven by reversible bimolecular motors, which are able to rotate the flagella in clockwise (CW) or counterclockwise (CCW) directions (Berg 1993). When all the flagella rotate in the CCW direction, they form a bundle, which propels the bacterium in one direction, which is generally referred to as a “run”. When one of the biomotors reverses and rotates CW, the associated flagellum separates from the bundle, and the bacterium moves erratically and reorients itself or “tumbles” (Kim et al. 2004). When cultured on a soft agar semi-solid surface, *S. marcescens* exhibit a different form of locomotion known as swarming. This type of locomotion is still based on propulsion by flagella, but the individual cells undergo a change in phenotype, elongating up to 10 μm and become hyperflagellated (Alberti and Harshey 1990). The extreme vigor of these cells is leveraged for the actuation technique described herein.

A need to develop a methodology to fabricate precise, consistent and well-defined microstructures of desired shape and size that can be individually manipulated into the working fluid provides the motivation for this work. Using the methodology described here, many additional studies on control techniques may be performed. One such

study is a letter on phototactic control of microstructures (Steager et al. 2007), though this brief did not detail the parameters involved with microfabrication, micromanipulation and actuation as encompassed here. Additionally, the geometric effect of microstructures powered by bacterial actuation is considered in an unrestricted, open-channel environment. Through a series of experiments with structures of varying geometry and aspect ratio, it is concluded that microstructure geometry plays no role in determining the mode of actuation (translation vs. rotation), but microstructure velocity is dependent on size.

2 Methods and materials

To accomplish effective actuation of custom designed microstructures several processes are necessary. These processes include culturing bacteria *S. marcescens* using the swarm plate technique, fabricating microstructures, blotting and manipulating microstructures with bacteria into the working fluid, and finally tracking the microstructures using an algorithm to quantify the magnitude and direction of motion.

2.1 Cell culturing

Swarming *S. marcescens* were cultured on a 0.6% agar plate. Swarming bacteria are especially useful as actuators due to their rigor and size. They are hyperflagellated, elongated and migrate cooperatively (Henrichsen 1972). The surface distribution of the swarm on the agar plate presents a flat, broad surface for the microstructure blotting technique presented in Sect. 2.3. To prepare agar plates for swarming, 5 g Difco Bacto tryptone, 2.5 g yeast extract, 2.5 g NaCl and 3 g Difco Bacto agar are dissolved in 500 ml deionized water. After autoclaving, the solution was poured into smaller bottles for later redistribution to Petri dishes. This solution will solidify when stored at room temperature and can be re-liquefied using a microwave on the lowest power setting. Before pouring individual agar plates, the agar solution was mixed with 25% glucose solution by adding 1 ml glucose solution for 100 ml of prepared agar solution. Fifty milliliters of this new agar solution was pipetted into large, 14 cm Petri dishes. The swarm plate on one edge was inoculated with 2 μl of *S. marcescens* saturated culture. Agar plates were incubated at 30–34°C, and swarming began within 8–16 h (Fig. 1). The inoculation site generally turned pink shortly after the swarming motion developed. The swarms expanded across the plate in waves that appeared as concentric rings with the most active bacteria along the outermost edge of the swarm.

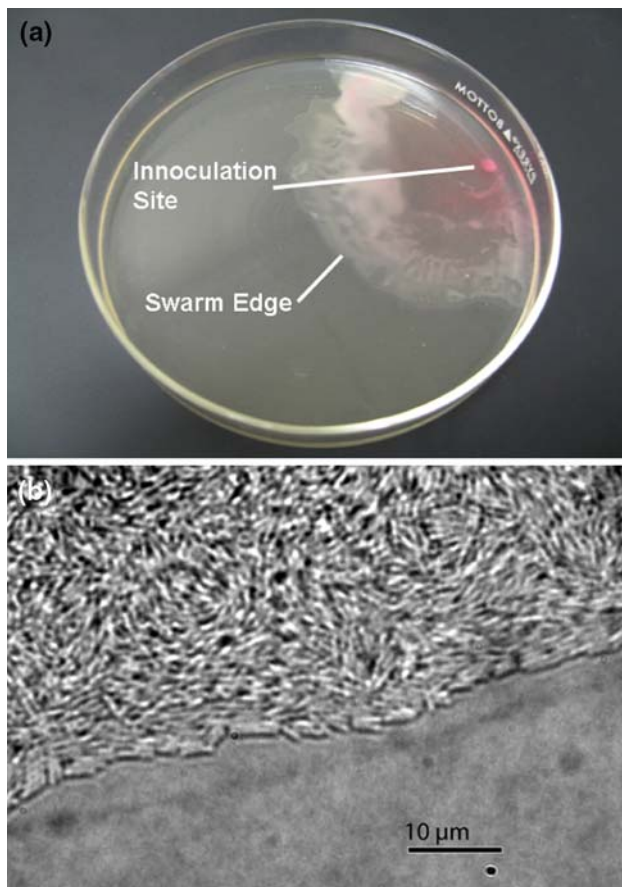


Fig. 1 **a** Appearance of 14 cm swarm plate 16 h after inoculation. Inoculation site near the edge appears as an opaque dot. Swarm edge has propagated roughly 7 cm. **b** Appearance of elongated *S. marcescens* along swarm edge

2.2 Microfabrication

Future studies and applications require precise microstructures that can be fabricated on large-scale, manipulated into the working fluid, and tracked using an algorithm with minimum processing time. To achieve these goals, fabricated structures should be biocompatible in the sense that materials preserve and promote bacterial motility and provide a surface to which bacteria attach readily. Additionally, the composite specific gravity of the structure should be similar to the working fluid and provide both chemical and thermal stability. It is additionally helpful if the fabricated structures are transparent and have a high refractive index to provide clearly defined boundaries, which can be readily discerned by a tracking algorithm.

2.2.1 Mask design

Masks are an integral component in the photolithographic process of microstructure fabrication. Using AutoCAD, the

designed two-dimensional micro-geometry was drawn with precision, and printed onto a transparency film (CAD/Art Service, Inc, Bandon, OR) with high resolution (18,000 dpi). A dark field mask design for microstructures was generated with three different geometries patterned on the wafer: squares, triangles and circles. These geometries were repeated on four quadrants of the circular wafer with different aspect ratios. In the second, third and fourth quadrants, the squares were extended to rectangles while the circles were extended to ellipses. The dimensions of the geometries designed on the mask were $50 \times 50 \mu\text{m}^2$ squares, $50 \times 100 \mu\text{m}^2$ rectangles, $50 \times 150 \mu\text{m}^2$ rectangles, $50 \mu\text{m}$ equilateral triangles, $50 \times 100 \mu\text{m}^2$ height isosceles triangles, $50 \times 150 \mu\text{m}^2$ height isosceles triangles, $50 \mu\text{m}$ circles, ellipses with minor axes of $50 \mu\text{m}$ and major axes of $100 \mu\text{m}$, and ellipses with minor axes of $50 \mu\text{m}$ and major axes of $150 \mu\text{m}$. The distance between each individual pattern was approximately $40 \mu\text{m}$ to allow working space for extraction of individual microstructures.

2.2.2 SU-8 microstructure fabrication

SU-8 Series 10 (MicroChem, Newton, MA) negative photoresist forms strong cross links on exposure to ultraviolet (UV) light, and the unexposed regions are easily removed using a developer solution. A two-inch silicon wafer was first cleaned in isopropanol. The wafer was then dried with nitrogen gas, rinsed with deionized water, and dehydrated at 200°C for 5 min. Once the wafer was pre-treated, it was placed on the vacuum chuck of a spin coater. SU-8 10 negative photoresist was dispensed on the wafer to cover two-thirds of the wafer surface or 1 ml per inch of diameter. In order to achieve a final thickness of $10 \mu\text{m}$, the spin coater was set to ramp to 500 rpm at 100 rpm/s, held for 5–10 s, and was ramped to a final spin speed of 3,000 rpm at 300 rpm/s, held for 30 s at that speed, and stopped gradually. Upon completion of this process, the wafer was soft baked in two steps. First, the wafer was pre-baked for 2 min at 65°C and then soft-baked at 95°C for 5 min. The next fabrication step was UV exposure. The total energy dose is $100\text{--}150 \text{ mJ/cm}^2$. On completion of exposure, the second step was to post-bake the wafer. During post-bake, the wafer was baked at 65°C for 1 min then shifted to another hot plate to be baked at 95°C for 2 min. Once the wafer was cooled, an SU-8 developer was used to wash away regions of unexposed SU-8 from the wafer and leave only the microstructures patterned on the surface. The wafer was submerged in a container with SU-8 10 developer for approximately 2 min. The container was gently agitated to allow complete removal of unexposed SU-8 10. Isopropyl alcohol was then applied to wash away any developer left on the surface of the wafer. This wafer

was once again rinsed with deionized water to remove any toxins that were present on the wafer. The wafer was then blow-dried with a jet of nitrogen gas, and the SU-8 pattern was ready for blotting and extraction (Fig. 2).

2.2.3 Microfabrication of silicon (Si) and polydimethylsiloxane (PDMS) microstructures

These experiments were also performed with polydimethylsiloxane (PDMS) microstructures which is the clear choice for biocompatibility; however, it was determined that individual PDMS structures were difficult to manipulate and control due to the adhesion of PDMS structures to all surfaces. This is a common difficulty in microassembly where traditionally neglected forces (electrostatic, van der Waals, surface tension) become dominating (Vandaele et al. 2005). Though successful trials with PDMS were completed, the successful yield of well-formed, free-floating PDMS structures was too low to allow collection of significant data.

PDMS microstructures were fabricated using an SU-8 mold, which was identical to the process used in Sect. 2.2.2. To prepare PDMS, Sylgard 184 silicon elastomer and its curing agent (Dow Corning, Midland MI) were mixed at a 10:1 mass ratio. This mixture was then degassed for 45 min to remove all embedded bubbles. After degassing, PDMS was spun on the SU-8 10 mold in a series of two cycles. During the first cycle, the glass wafer was accelerated from rest to 2,200 rpm at an acceleration of 550 rpm/s and held at this speed for 30 s to evenly spread the PDMS across the surface. For the second process, the wafer is further accelerated at 2,500–5,000 rpm and maintained at this speed for another 30 s to obtain a thin layer of PDMS over the mold surface. The remaining PDMS then cured at 100°C for 1 h.

In addition to SU-8 and PDMS microstructures, pure silicon may also be patterned using silicon-on-insulator (SOI) wafers (Madou 1997). Microstructure geometry is defined by masking individual structures with positive photoresist. The sidewalls are etched using reactive ion etching (RIE) and structures using buffered oxide etch (BOE).

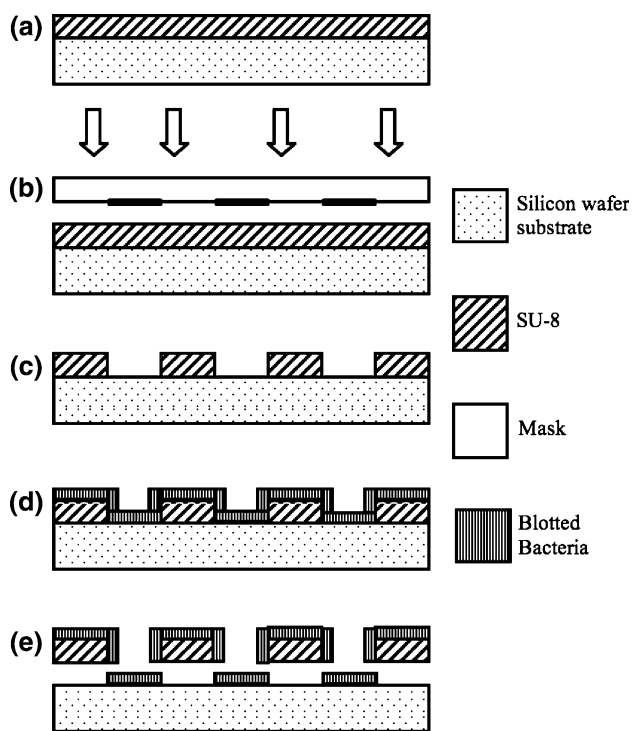


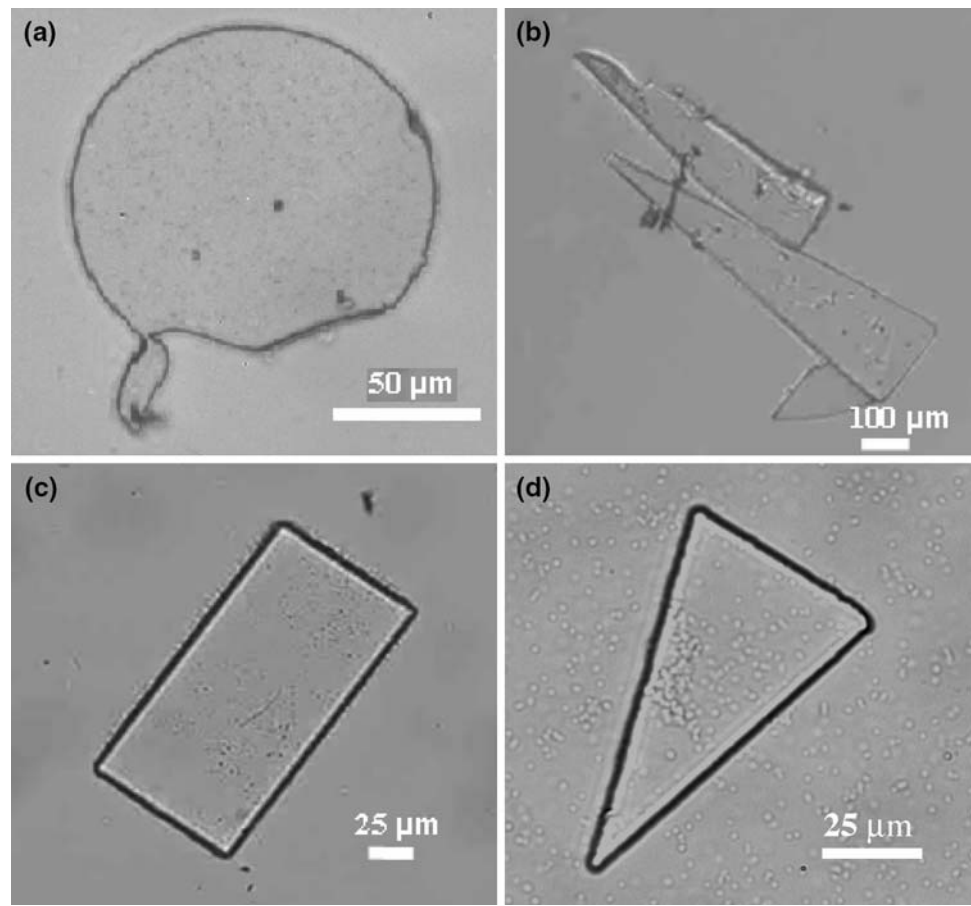
Fig. 2 Microfabrication of SU-8 microstructures. **a** The silicon wafer is coated with SU-8 10 photoresist. **b** UV light is transmitted through a photomask to create an exposure pattern. **c** SU-8 developer is used to remove uncrosslinked photoresist. The wafer is rinsed in isopropanol and DI water and dried with nitrogen. **d** Sections of the wafer, each with many microstructures, are inverted along the swarm edge for bacterial attachment. **e** Individual microstructures are mechanically released into motile buffer

2.2.4 Advantages of SU-8 over PDMS and silicon microstructures

It was observed that bacteria attached readily to negative photoresist SU-8 series 10. SU-8 has good chemical and thermal resistance, and its high optical transparency is well suited for image processing. SU-8 has a refractive index of 1.68 (Ling and Lian 2006) as compared to PDMS and Si has a refractive index 1.41 (Vezenov et al. 2005) and 0, respectively. The higher the refractive index of a substance, the greater the light bends at the surface interface, in this case motile buffer and SU-8 microstructures. This is important from the point of view of the tracking algorithm because transparent substances with higher refractive indices (SU-8) tend to create a well-defined boundary under a microscope (Fig. 3) than substances with lower refractive indices (PDMS). Clearer structure outlines allow a reduction in processing time due to the high edge contrast.

Additional advantages of SU-8 microstructures are based on mechanical properties. SU-8 shows good adhesion to silicon during the fabrication process, but what is particularly useful about SU-8 is that once released from substrate it does not immediately reattach to the substrate surface or working instruments. This property of SU-8 makes it a perfect candidate for bacterial actuation studies, allowing the structures to adhere well to the silicon chip during the fabrication and blotting process yet still be easily removed and manipulated. On the other hand, PDMS

Fig. 3 Ten micrometers thick PDMS and SU-8 structures. **a** PDMS tears very easily under micromanipulation and **b** exhibits adhesive forces to other PDMS structures, working tools, and the Petri dish. **c** SU-8 demonstrates higher rigidity and ability to more easily micromanipulate. **d** The higher index of refraction of SU-8 also creates higher background contrast



consistently adheres to all surfaces including working instruments before and after the fabrication and blotting process, which makes it difficult to release individual PDMS structures into the working fluid for experimentation. Where it takes seconds to successfully remove and manipulate many SU-8 structures, it takes 1–2 h to manipulate a single PDMS microstructure.

Flexible PDMS microstructures with a low Young's modulus (750 KPa) (Lotters et al. 1997) were seen to tear during manipulation processes. Using SU-8 microstructures with a high Young's modulus (4.02 GPa) (Lorenz et al. 1997) made the extraction process easier with little or no structural damage to the microstructures and neighboring structures. The flexible, adhesive, and elastic nature of PDMS additionally limited the microstructure size that could be extracted to roughly 300 μm in the greatest dimension. Additionally, the transition in the fabrication material from PDMS to SU-8 led to easier simultaneous removal of a number of microstructures from the silicon wafer. As seen in Fig. 3, SU-8 microstructures had stronger integrity than PDMS microstructures, and could be easily extracted without damage. SU-8 was strong enough to withstand micromanipulation processes, but at the same time was easily separable from the silicon wafer substrate.

Silicon presents a favorable substrate for bacterial adhesion and actuation; however, there are significant disadvantages. Primarily, the cost of the fabrication procedure is several times higher than that for SU-8 structures. Since silicon is not transparent, it is impractical to determine the efficacy of the blotting process. An evaluation of the bacterial monolayer is important to gain an understanding of structure motion, and this important step is difficult with opaque materials since bacterial cell bodies are only clearly apparent using phase contrast microscopy.

2.3 Micromanipulation

Current research depends on sophisticated, expensive equipment to perform micromanipulation. Considering that future application implementing bacterial actuators will require simpler, inexpensive micromanipulation process, a series of steps was developed to release microstructures into the working fluid without damaging the structure or attached bacteria. Henceforth, micromanipulation will be referred to as a procedure by which microstructures blotted with bacteria are extracted from the substrate and released into the working fluid with the aid of the microscope.

After the fabrication process, the 2-inch wafer with microstructures was cut into sections of 10×5 mm using a diamond tipped engraving pen, which contained several fully intact microstructures. To blot, the separated sections were washed with motility buffer (0.01 M potassium phosphate, 0.067 M sodium chloride, 10^{-4} M ethylenediaminetetraacetic acid (EDTA), 0.01 M glucose, and 0.002% Tween-20, pH 7.0) then inverted onto the edge of the swarm plate. The section was removed from the swarm plate, transferred to a dish with motility buffer, and lightly agitated to remove unattached bacteria and excess agar. This process ensured that a monolayer of bacteria was attached to the microstructures with flagella free to move and untangled from other layers of bacteria and agar. The blotted section was then moved to a fresh Petri dish and submerged under a thin layer of motility buffer. The manipulation was performed using a stereomicroscope for three-dimensional viewing, thus allowing individual microstructures to be selected and removed. As seen in Fig. 4, after affixing the silicon chip to the bottom of the Petri dish, a 25-gauge needle was used to select and remove structures along the longest side. The flat side of the end of the needle, rather than the pointed tip was used for removal. This allowed the force that is required to break

the structure from the substrate to be evenly distributed thus minimizing deformation caused by point loads.

2.4 Microstructure tracking

A tracking algorithm was designed to analyze the motion of the SU-8 microstructure driven by the attached flagellated bacteria *S. marcescens* in motility buffer. The current study analyzed two distinct motions of rigid bodies, translation and rotation. To characterize the motion of the bacteria-driven microstructures, the geometric centroid and orientation angle was traced. The algorithm was validated by testing the motion and velocity of a theoretical test structure with predetermined shape and velocity. A set of consecutive frames with $2,048 \times 2,048$ pixels were captured using a Retiga 4000R digital camera and imported into MATLAB for analysis.

The analysis involved four main steps: pre-processing, image enhancement, structure recognition, and calculation of centroid and velocity (Fig. 5). In the pre-processing stage, the brightness levels at the microstructure boundary and time interval between the frames were found using image processing software, ImageJ (NIH). The matrix of 2,048 column and 2,048 rows was created to hold the brightness value for each pixel of $2,048 \times 2,048$ frames. In image enhancement stage, a set of conditional loops scanned each and every pixel, both length- and width-wise, to make the pixels at the boundary completely black, to remove the unwanted gray background surrounding the structure and to remove black pixels within and surrounding the boundary to distinguish the structure from bacteria and other unwanted noise in the image. Stranded black pixels around the microstructure that were not part of the structure were also removed by detecting and removing every black pixel or structure, below a $5 \mu\text{m}$ size. After image enhancement, the next processes were structure recognition and velocity calculation. Structures were recognized using a vertical scan that detected and recorded the upper and lower boundary of the structure in each column.

The shape of the microstructure was recognized by both vertical and horizontal scans, giving the x - y coordinates of each pixel constituting the upper and lower boundaries of the isolated microstructure. When the centroid of the shape was calculated, the shape was divided into a combination of known shapes which are lines ending up with upper and lower boundary pixels, then the following formulae were applied,

$$x_c = \frac{\sum A_i x_i}{A_{\text{total}}}, \quad y_c = \frac{\sum A_j y_j}{A_{\text{total}}} \quad (1)$$

where x denotes the direction of the image length and y the image width, x_c and y_c denote the coordinates of the

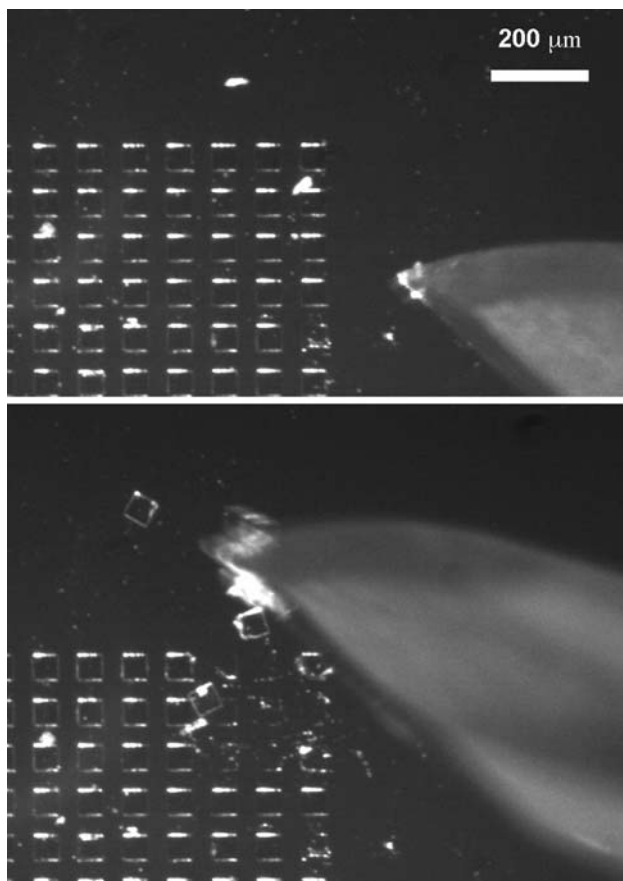
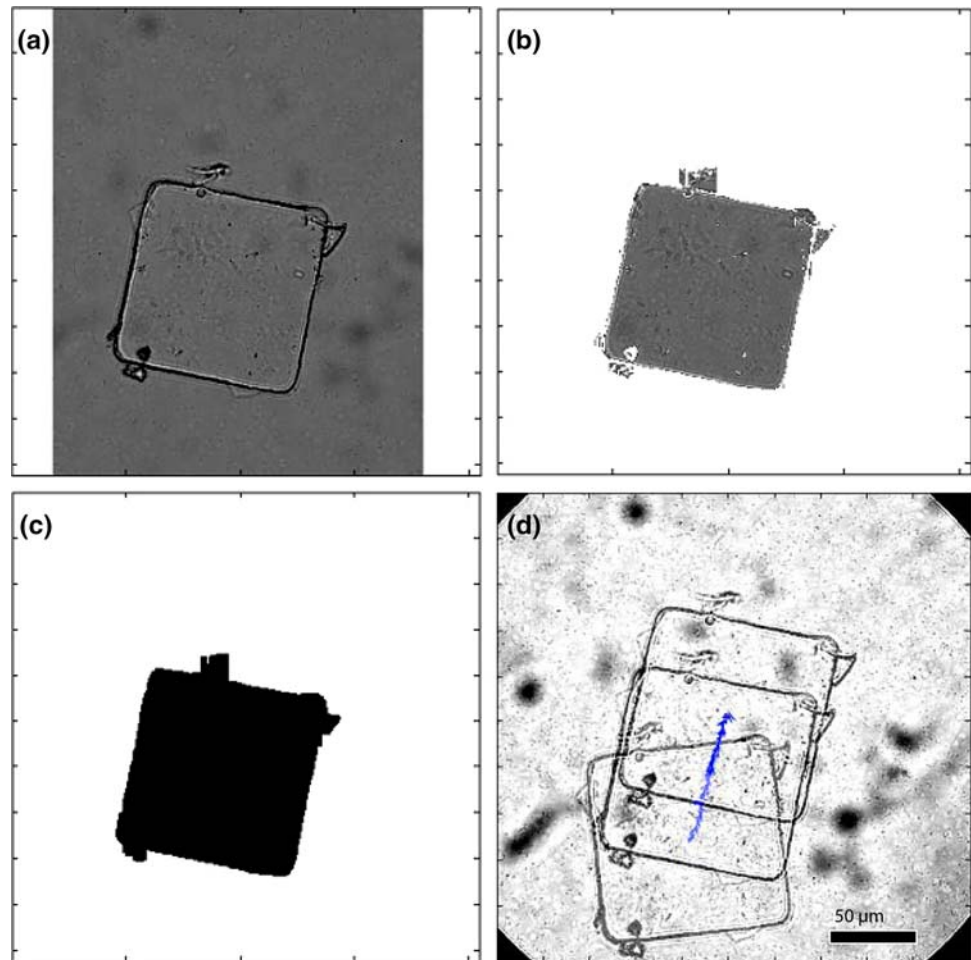


Fig. 4 Extraction of $50 \mu\text{m}$ square SU-8 structures

Fig. 5 Structure tracking.
a Individual video frames of 100 μm square structure movement is captured.
b An edge detection routine is used in each frame of video to isolate the structure.
c The image is converted to a binary image for measurement of centroid and angle.
d A progressive vector map of the centroid velocity is superimposed on a time lapse series of images from the original video



centroid of the microstructure, A_i and A_j represent the area of sub-shapes composing the microstructure, x_i and y_i are the coordinates of the centroid of the sub-shapes, and A_{total} is the total area of the microstructure. The distance between the centroids of the consecutive frames was calculated based on the pixel-to-pixel distance, which corresponded to the appropriate viewing magnification, allowing the magnitude and direction of the microstructure motion to be calculated and plotted.

3 Experimental results

It has been observed in various applications including microfluidic pumps (Kim and Breuer 2005) and phototactic control of autonomous microstructures (Steager et al. 2007) that bacteria can generate useful work from self-organized global coordination amongst the flagella that form the bacterial carpet. Closed systems studies on bacterial carpets show that boundary conditions have a significant impact on bacterial behavior and hence its coordination. Therefore, it was important from the control point of view to know how

the microstructures blotted with bacterial carpets would perform in open channels with no sidewall boundary conditions. Based on studies concerning swarming bacterial behavior (Dombrowski et al. 2004) and the behavior of blotted bacterial carpets, the authors designed and fabricated structures with different geometries and aspect ratios to test the hypothesis that microstructures with different geometric shapes produce some preferential directional motion in the open channel. Bacterial carpets have been observed to produce local regions of translational and rotational fluid motion, referred to as rivers and whirlpools. The average interwhirlpool distance is 30 μm , and the location of whirlpools centers shift, merge, and dissipate within 10 min (Darnton et al. 2004). If there existed a relation between geometry and directional motion, structural shape would play an important role in deciding the shape of mechanical parts in the bacterial actuated microsystems.

It should be noted that care was taken to assure that microstructure motion was independent of all external stimuli. Considerable settling time was allowed after addition of motile buffer. Bacteria and particles in the local

fluid field were compared to assure that results were not part of a larger bulk flow. Hydrostatic effects are also not a factor since all experiments were performed in a Petri dish that was leveled with respect to the level surface of a vibration isolation table. Microstructures were completely submerged and generally within 5 μm of the Petri dish surface. The depth of the fluid was 4–5 mm. Structures were intentionally kept close to the surface of the Petri dish to avoid bulk flow due to thermal and evaporative effects.

After a series of experiments with various structures, it is concluded that geometry of the microstructure plays no role in creating a resultant translational or rotational motion in an open channel. As shown in Fig. 6, both translation and rotational motions were observed with clockwise and anticlockwise rotational motion being dominant. In a carpet of densely packed cells, the interactions between many flagella in a neighborhood leads to the formation of local pockets of coordinated fluid motion (Kim and Breuer 2007). It is inferred that rotation or translation motion are the result of the size of coordinated regions and their alignment. When size is limited, net thrust is generated in one direction. The clear exception to this occurs when bacteria are blotted unevenly. For instance, if bacteria are blotted only along one edge of a structure and coordinate in a direction tangential to the center, rotation will dominate (Fig. 7). It was observed that as size increases, velocity of the structure decreases and more rotational motion was predominant. The structures studied with the smallest dimensions showed the highest rate of translation (15 $\mu\text{m/s}$) and rotation (3.1 rad/s). A summary of results for different materials, dimensions and their corresponding modes of motion are given in Table 1. For larger structures on the scale of 50–100 μm , the bacterial carpet naturally divides into separate competing regions in which the flagella of each region are coordinated and aligned in one direction. Without sidewall boundary conditions these regions have a tendency to create a net torque generating a resultant rotational motion. In the absence of the coordination, the widths of the coordinated regions are smaller with all the individual regions pointing in different direction creating a zero resultant motion. A directional stimulus such as magnetotaxis (Martel et al. 2006), galvanotaxis (Adler and Shi 1988), or phototaxis could be used to direct these individual forces/regions generating a directed and controlled translational or rotational motion. The MATLAB algorithm that was demonstrated in Sect. 2.4, could be used as a feedback component to adjust the stimulus to keep the microstructure on a predetermined track. The systems can be sustained for hours or even days if nutrient supply and environmental conditions are maintained.

Considering that this work was exclusively performed in the open channel, future work will focus on the effects of adding boundary conditions to determine if geometry has a

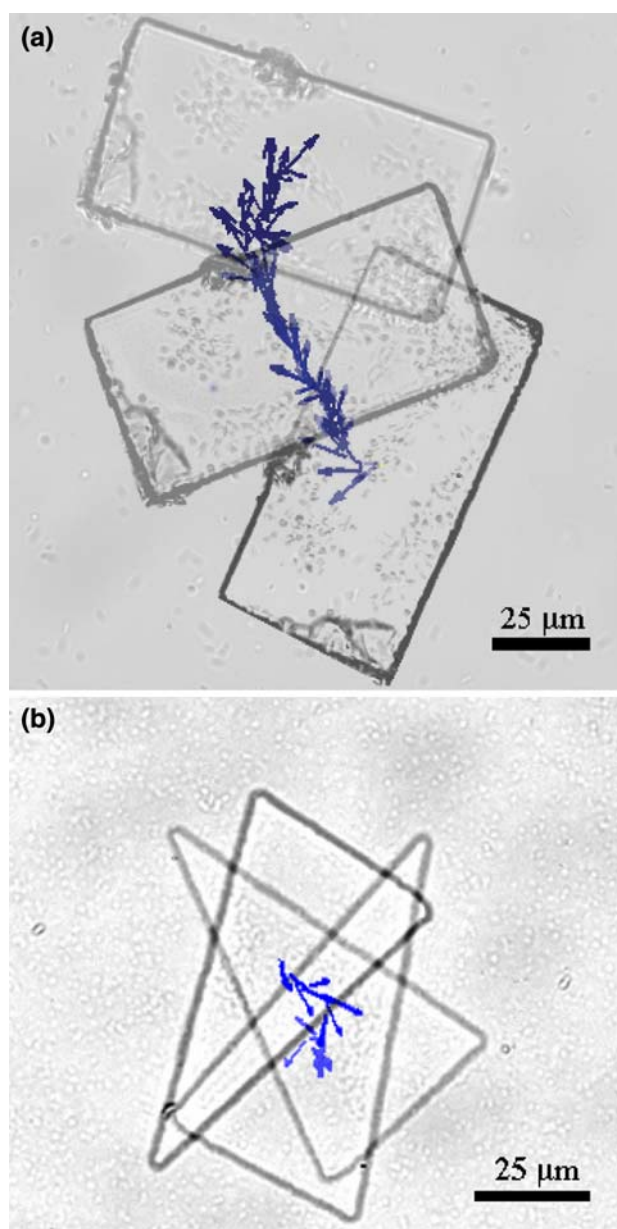


Fig. 6 Velocity vectors show centroid movement. **a** A $50 \times 100 \mu\text{m}$ rectangular barge translates at an average speed of $1.7 \mu\text{m/s}$ during 25 s and rotates 1.48 radians. **b** A $50 \times 100 \mu\text{m}$ isosceles triangle rotates 3.1 radians during 50 s with centroid translating at an average speed of $1.9 \mu\text{m/s}$

greater influence on structure motion in a more restricted environment. Microstructure motion will be studied in closed microfluidics channels of width only, slightly larger than the structures themselves. This will be accomplished by studying motion due to bacteria actuation in confined microfluidic channels of varying geometry.

Although it has been suggested that typical speed should be roughly independent of size (Darnton et al. 2004), this work suggests that there may be additional factors to consider. This is most easily understood by considering the

Fig. 7 Silicon microstructure rotating at a consistent angular velocity of 3.7 rad/s. Rotation persisted for several minutes. Centroid velocity averaged 15 $\mu\text{m/s}$

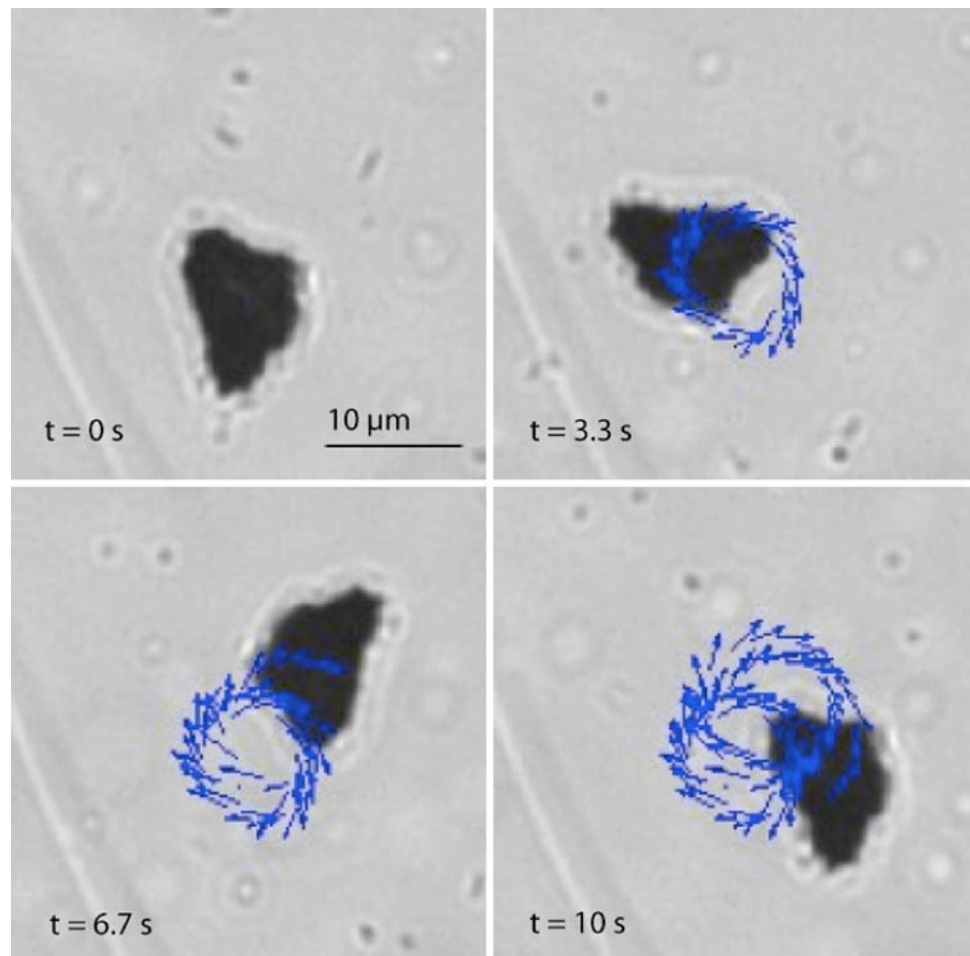


Table 1 Comprehensive data showing the relation of microstructure size to that of velocity

Scale (μm)	Material	Velocity ($\mu\text{m/s}$)	Modes
5–15	Silicon	4–15	Helical/rotational
50–100	SU-8/PDMS	1.5–2.5	Translational/rotational
200–400	SU-8	$\ll 1$	Rotational

upper and lower limits of practical structure size. At the upper limit for structures on the scale of 400 μm , it has been observed that bacteria are unable to generate sufficient coordination to induce a propulsive force on the microstructure. For the lower limit, a structure similar in size to the bacterial cell body can be considered. In this case, the combined radius of the structure and cell body is only slightly greater than the cell body itself. The combined Stokes' drag estimation in this case is very similar considering that the combined effective radius is only slightly increased, thus it is expected that the overall velocity of propagation will be quite similar to the velocity of a free-swimming bacterium. Indeed, this increase in velocity has been experimentally observed (Figs. 7, 8) by

studying the motion of structures less than 10 μm in greatest dimension. Additionally, it is more likely that bacteria in very close proximity will coordinate in the same direction.

Lastly, it should be noted that material selection is extremely important for these observations. PDMS and SU-8 structures have specific weights very similar to that of the fluid environment (1.05 g/cm^3 , 1.2 g/cm^3 , respectively). This limits the effects of gravity on the ability of bacteria to actuate microstructures. This is also the reason that the only observations with silicon chips (density 2.33 g/cm^3) that have been made have been with the smallest of dimensions. Thick (greater than 4 μm) silicon structures cannot be propelled due to the overwhelming effect of gravity.

4 Conclusion

This work was designed to develop more effective methods to study bacterial actuation systems by exploring various microfabrication, manipulation and tracking techniques. Using the methodology described here, microstructures of custom design may be used to develop many novel studies

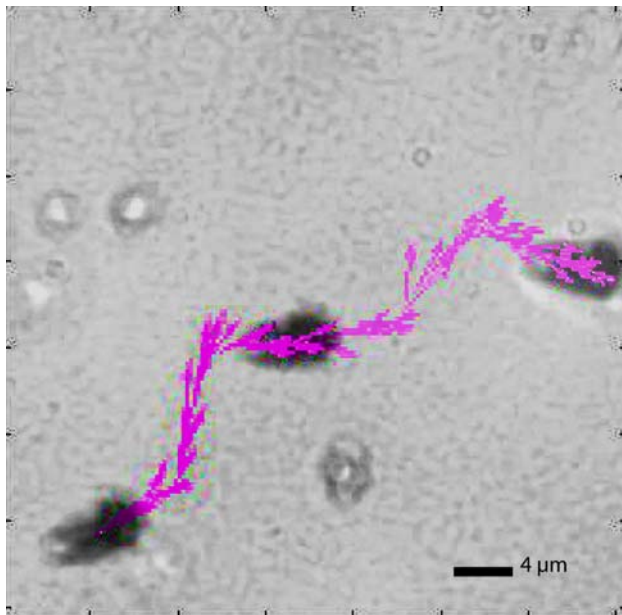


Fig. 8 Time lapse image of $8 \times 4 \mu\text{m}$ silicon chip helical motion with velocity $4.4 \mu\text{m/s}$. Image appears blurred due to three dimensional rotation in and out of focal plane. Helical motion continued for several minutes

in the area of microorganic actuation and control. It was discovered that use of SU-8 and silicon for actuation of structures of repeatable geometry were favorable over employing PDMS. Results concerning geometric influence on structure trajectory also showed that while the mode of structure propagation (translation vs. rotation) was more or less independent of shape, mean velocity increases as structure size decreases. Further study will determine how the mode of propagation and velocity are related to patterns of bacterial blotting.

These methods may be applied to many additional studies concerning bacterial actuation systems as various experimental parameters are explored. Also, it is thought that the nature of flagellar orientation and activity may be demystified using these techniques for the development of more effective bacterial transportation systems. The planar nature of microfabrication and bacterial blotting nicely matches the restriction of light microscopy to observation in a single plane at one time.

Further experimentation will focus on developing reliable control mechanisms for the concept of a biofactory. That is, bacterial actuation will be used as a method of micromanipulation for the assembly of larger microstructures composed of many parts. The structure-tracking algorithm will ultimately be optimized as a feedback element within bacterial actuation control schemes.

Acknowledgments The authors acknowledge the invaluable contributions of Svetlana Rojevskaia, Linda Turner, and Howard Berg for access to their bacteria strains, their expertise, and experience in

culturing and handling *S. marcescens*. Special thanks go to Kenny Breuer and Siran Manoleehagul for their useful conversations. The authors would additionally like to acknowledge Rafael Mulero, Chandan Naik, Sochet Bith, Lindsay Reber and Michael Johnson for their suggestions, contributions and insightful discussions. This work was supported by Drexel start-up funds and in part by NSF No. DGE-0538476.

References

- Adler J, Shi W (1988) Galvanotaxis in Bacteria. Cold Spring Harb Symp Quant Biol LIII:23–525
- Alberti L, Harshey RM (1990) Differentiation of *Serratia marcescens* 274 into swimmer and swarmer cells. J Bacteriol 172:4322–4328
- Behkam B, Sitti M (2007) Bacterial flagella-based propulsion on/off motion control of microscale objects. Appl Phys Lett 90:023902
- Berg HC (1993) Random walks in biology. Princeton University Press, NJ
- Berg HC (2003) E. coli in motion. Springer, Berlin
- Darnton N, Turner L, Breuer KS, Berg HC (2004) Moving fluid with bacterial carpets. Biophys J 86:1863–70
- Dombrowski C, Cisneros L, Chatkaew S, Goldstein RE, Kessler JO (2004) Self-concentration and large-scale coherence in bacterial dynamics. Phys Rev Lett 93:098103
- Eringen A (1964) Simple microfluids. Int J Engrg Sci 2:205–217
- Gal-El-Hak M (1999) The fluid mechanics of microdevices—the freeman scholar lecture. J Fluid Eng 121:5–33
- Henrichsen J (1972) Bacterial surface translocation. Bacteriol Rev 36:478–503
- Ho C, Tai Y (1998) Micro-electro-mechanical-system (MEM) and fluid flows. Annu Rev Fluid Mech 30:579–612
- Kim MJ, Breuer KS (2005) Characteristics of bacterial pumps in microfluidic systems. In: 2005 NSTI-nanotechnology conference and trade show, Anaheim, CA, pp 712–715
- Kim MJ, Breuer KS (2007) Self-organizing bacteria-powered microfluidic pumps. Small (in press)
- Kim MJ, Kim MJ, Bird JC, Park J, Powers TR, Breuer KS (2004) Particle image velocimetry experiments on a macro-scale model for bacterial flagellar bundling. Exp Fluids 37:782–788
- Ling Z, Lian K (2006) SU-8 3D microoptic components fabricated by inclined UV lithography in water. Microsyst Technol 13:245–251
- Lorenz H, Despont M, Fahrni N, LaBianca N, Renaud P, Vettiger P (1997) SU-8: a low-cost negative resist for MEMS. J Micromech Microeng 7:121–124
- Lotters J, Olthuis W, Veltink PH, Bergvel P (1997) The mechanical properties of the rubber elastic polymer polydimethylsiloxane for sensor applications. J Micromech Microeng 7:145–147
- Madou M (1997) Fundamentals of microfabrication. CRC Press, NY
- Martel S, Tremblay CC, Ngakeng S, Langlois G (2006) Controlled manipulation and actuation of micro-objects with magnetotactic bacteria. Appl Phys Lett 89:233904
- Steager E, Kim C-B, Patel J, Bith S, Naik C, Reber L, Kim MJ (2007) Control of microfabricated structures powered by flagellated bacteria using phototaxis. Appl Phys Lett 90(26):263901
- Vandaele V, Lambert P, Delchambre A (2005) Non-contact handling in microassembly: acoustical levitation. Precis Eng 29:291–505
- Vezenov DV, Mayers BT, Wolfe DB, Whitesides GM (2005) Integrated fluorescent light source for optofluidic applications. Appl Phys Lett 86:041104
- Weibel DB, Garstecki P, Ryan D, DiLuzio WR, Mayer M, Seto JE, Whitesides GM (2005) Microoxen: microorganisms to move microscale loads. Proc Natl Acad Sci USA 102:11963–11967